Stochastic Modeling of Lift and Drag Dynamics to Obtain Aerodynamic Forces with Local Dynamics on Rotor Blade under Unsteady Wind Inflow

MUHAMMAD RAMZAN LUHUR*, JOACHIM PEINKE**, AND MATTHIAS WAECHTER***

RECEIVED ON 17.05.2013 ACCEPTED ON 11.09.2013

ABSTRACT

This contribution provides the development of a stochastic lift and drag model for an airfoil FX 79-W-151A under unsteady wind inflow based on wind tunnel measurements. Here we present the integration of the stochastic model into a well-known standard BEM (Blade Element Momentum) model to obtain the corresponding aerodynamic forces on a rotating blade element. The stochastic model is integrated as an alternative to static tabulated data used by classical BEM. The results show that in comparison to classical BEM, the BEM with stochastic approach additionally reflects the local force dynamics and therefore provides more information on aerodynamic forces that can be used by wind turbine simulation codes.

Keywords: **Wind Tunnel Measurements, Unsteady Wind Inflow, Stochastic Model, Lift Dynamics, Drag Dynamics, Blade Element Momentum Method, Local Force Dynamics.**

1. INTRODUCTION

The dynamic nature of the wind contributes to the complex operation of wind turbines being exposed to turbulent atmospheric air flows having well-known complex statistics and gusty behavior [1-3]. The operation of wind turbines in such environment leads to several risks especially in terms of highly dynamic mechanical loads [4-5]. Several studies exist on placing an airfoil into a steady low-turbulence inflow and observing the lift and drag properties at constant AOAs (Angles of Attack) [6-9], however, the complexity of open-air turbulent flows is yet to be perceived fully.

The blade aerodynamics under turbulent wind conditions changes profoundly compared to steady low-turbulence flows. In unsteady flow the fast variations in AOA can lead to well-known dynamic stall effect resulting in significant increase in lift dynamics, compare [10-12].

To estimate the aerodynamic forces on wind turbine rotor blades several engineering and CFD (Computational Fluid Dynamics) techniques exist today [1,13-16]. However, from performance point of view still engineering methods are the leading choice over CFD [17]. CFD yet needs more powerful computers to achieve acceptable computational time [18]. Still most wind turbine aerodynamic computations are performed with standard BEM method due to its simplicity and computational efficiency in particular [18].

*Ph.D. Researcher, **Professor, and ***Post-Doctoral Researcher,
ForWind-Centre for Wind Energy Research, University of Oldenburg, Germany.

Nevertheless, most of the aerodynamic models use tabulated static data for an airfoil at constant AOAs [19-20] to estimate the forces on wind turbine blades, and therefore lack the information on the local dynamics.

In this work, a stochastic model of the lift and drag dynamics is integrated into a classical BEM as an alternative to static airfoil data table to obtain the aerodynamic forces with complete local dynamics. The model evaluates the lift and drag forces numerically as function of AOA. The forces are obtained for a rotating blade element and are compared with results obtained with classical BEM (with the use of static airfoil data table). The model is being developed to extract and provide the detailed local loading information acting on the wind turbine blades which could lead to an optimum rotor design under turbulent wind conditions. The final goal is to achieve an aerodynamic model like AeroDyn [19] based on stochastic approach. Later it could be combined with a wind energy converter model to obtain a stochastic rotor model.

The paper is structured as follows. Section 2 describes the lift and drag modeling approach. Section 3 explains the calculation of rotor normal and tangential forces for a blade element in the context of classical and stochastic BEM (with model addition) methods. Section 4 presents the results from both the classical and the stochastic BEM approaches. Finally section 5 concludes the outcome.

2. STOCHASTIC LIFT AND DRAG MODEL

The stochastic modeling of lift and drag dynamics is consisting of two steps. First, measurements have been performed in wind tunnel to obtain the airfoil data. Second, a stochastic approach is applied with an optimization scheme to model the lift and drag dynamics.

2.1 Measurements

The measurements have been performed in a closed loop wind tunnel of Oldenburg University for an airfoil FX 79-W-151A having chord length of 0.2m. The wind tunnel has a test section of 1m wide, 0.8m high and 3m long. The turbulent inflow was generated using a fractal square grid having closer characteristics to natural wind [21-22]. The lift and drag forces were measured directly using two strain gauge force sensors fixed at the end points of an airfoil in span-wise direction as shown in Fig. 1. The mean wind velocity and Reynolds number were 50m/s and $7x10^5$ respectively. Further details of the measurement can be found in [22].

2.2 Stochastic Modeling

The lift and drag coefficients are modeled using a stochastic approach which extracts most of the information available in the system dynamics. First, lift and drag coefficients are calculated from measured data using the relations [22]:

$$C_L = \frac{F_L}{qA} \tag{1}$$

$$C_L = \frac{F_D}{qA} \tag{2}$$

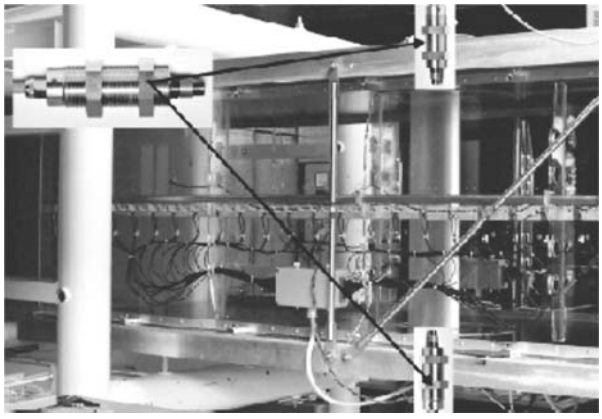

FIG. 1. VIEW OF THE WIND TUNNEL TEST SECTION. BLACK ARROWS SHOW THE POSITION OF FORCE SENSORS INSTALLED AT THE END POINTS OF VERTICALLY MOUNTED AIRFOIL IN THE TEST SECTION

Where F_L is the lift force, F_D the drag force, q the inflow dynamic pressure and A the area of the airfoil.

The stochastic approach is applied on the measured time series of lift and drag coefficients using a first order stochastic differential equation called the Langevin equation, cf. [23]. The approach is based on drift and diffusion functions coupled with a noise term. It models the complex statistics by means of random numbers. The approach reads:

$$\frac{dX(t)}{dt} = D^{(1)}(X) + \sqrt{D^{(2)}(X)}.\Gamma(t) \tag{3}$$

Where $\Gamma(t)$ is a Gaussian white noise termed as Langevin force [23] with mean value of $\langle\Gamma(t)\rangle$=0 and variance $\langle\Gamma^2(t)\rangle$=2. It is an uncorrelated statistical noise obeying the PDF (Probability Density Function) of normal distribution.

The $D^{(1)}(X)$ and $D^{(2)}(X)$ are the drift and diffusion functions, also known as first and second Kramers-Moyal coefficients for $X(t)$. The drift and diffusion functions can be estimated from measured time series using the relation [24-26]:

$$D^{(1)}(X,\alpha)_{n=1,2} = \lim_{\tau\to 0}\frac{1}{n!\,\tau}\left\langle \left(X(t+\tau)-X(t)\right)^n \right\rangle \Big|_{X(t)=X,\alpha} \tag{4}$$

Where X represents the lift and drag coefficients, α the fix AOA, $D^{(1)}(X,\alpha)$ the drift function and $D^{(2)}(X,\alpha)$ the diffusion function. The drift function represents the deterministic part of the system and estimates the mean time derivative of the $X(t)$ whereas the diffusion function quantifies the amplitude of the stochastic fluctuations.

The direct estimation of $D^{(1)}(X,\alpha)$ and $D^{(2)}(X,\alpha)$ from Equation (4) may suffer from different sources of errors like finite sampling deviations, additional measurement noise etc. [22-28]. The Langevin Equation (3) is mainly dependent on these two functions which means quality of results strongly depend on the correct estimation of drift and diffusion functions. For this purpose, an optimization approach based on χ^2 test is applied on PDFs of the model and measured data. The χ^2 value is obtained as:

$$\chi^2 = \sum_i \frac{\left(p_{Model,i} - p_{Measure,i}\right)^2}{\left(p_{Model,i} + p_{Measure,i}\right)} \tag{5}$$

Where p_{Model} and $p_{Measure}$ are the stationary PDFs of model and measured data respectively. The χ^2 test quantifies the difference between the model and measured data sets. The lower the difference the better the quality of the results. Since the Langevin Equation (3) is random by nature due to involvement of the noise term, so it would be time-consuming to get the stable values by numerical simulation. As an alternative, the stationary PDF of the Langevin equation is used, which is known in its analytical form [23]:

$$p(X_{Model}) = \frac{N}{D^{(2)}(X_{Model})}\exp\left[\int^{X_{Model}}\frac{D^{(1)}(y)}{D^{(2)}(y)}\,dy\right] \tag{6}$$

Where N is a normalization factor.

For best estimation of drift and diffusion functions in an automatic way, the optimization approach described in Equation (5) is coupled with an interval sectioning procedure based on the Inverse Parabolic Interpolation algorithm [28]. The analytical expression for the algorithm is:

$$x = b - \frac{1}{2}\frac{(b-a)^2\left[f(b)-f(c)\right]-(b-c)^2\left[f(b)-f(a)\right]}{(b-a)\left[f(b)-f(c)\right]-(b-c)\left[f(b)-f(a)\right]} \tag{7}$$

Where x is the abscissa value of new estimated point and accounts for diffusion function here. The corresponding ordinate value of this new point is the χ^2 value. The a, b, and c are the abscissa values of the three randomly selected points and $f(a)$, $f(b)$ and $f(c)$ are the respective ordinate values of the three points along the inverse parabolic line. The algorithm works in a way that it discards one point after each iteration and decides for a new set of three points for next iteration like the point with minimum ordinate value is always in the middle of the three points. The algorithm continues for several iterations until the best value for x is obtained and thereafter stops functioning automatically as the points coincide with each other.

The basic model (Equation (3)) has been extended to incorporate for additional effects to reproduce satisfactory conditional PDFs $p(X(t+\tau)\,|\,X(t))$ for all time lags τ. These additional effects include out of phase lift and drag coefficients oscillation and the amplitude modulation (breathing) observed in the lift and drag coefficients time series. The extended model reads [29]:

$$X_{Model}(k) = X_{Langevin}(k) + A\sin\left(\frac{2\pi k}{T}\right)\exp\left[\left(\frac{-k'}{k_o}\right)^{S}\right] \quad (8)$$

Where $X_{Langevin}$ is the result obtained from Equation (3), A the constant to fix the oscillation amplitude for lift and drag coefficients, k the discrete time variable and T the most dominant oscillation period observed in the measured data time series. The exponential function in the equation controls the amplitude modulation of the oscillation along the lift and drag time series, where k_o is half the length of average breathing, $k' = (k \bmod k_o)$ and S is described as:

$$S = \begin{cases} +1, & for\ (2n)k_o < k \le (2n+1)k_o \\ -1, & for\ (2n+1)k_o < k \le 2(n+1)k_o \end{cases} \quad (9)$$

Where $n = 0, 1, 2, \ldots$

To correct for extension in Equation (8), once again an optimization approach is repeated. This time the stationary PDFs for model used in Equation (5) are taken from results of Equation (8) and the final obtained value of χ^2 is compared with intrinsic standard error to verify the quality of results. The relation for intrinsic standard error reads [2]:

$$S_{Error} = \sum_i \frac{\sqrt{N_i}}{N_{Total}} \quad (10)$$

Where N_i is the number of counts in the i^{th} bin and N_{Total} the size of the sample. For the best quality of the model, the χ^2 value is to be in order or less (in magnitude) than the standard error. Further details of the described model can be found in [29].

3. ESTIMATION OF ROTOR NORMAL AND TANGENTIAL FORCES

The rotor normal and tangential forces are estimated for a blade element using both the classical and stochastic BEM approaches. In classical BEM the static airfoil data table (which contains mean lift and drag coefficients as function of AOA obtained by measurements) is used as an input to BEM, whereas in stochastic BEM the model Equation (8) is integrated to BEM. The BEM model taken here is described in following section.

3.1 BEM Model

The rotor blade element forces are estimated with a well-accepted standard BEM model used in aerodynamic rotor model AeroDyn of the National Renewable Energy Laboratory [19]. To determine the aerodynamic forces, it

is necessary to first calculate the inflow angle to obtain the effective AOA on the rotating blade element. The expressions in this context are [19,30]:

$$\tan\phi = \frac{V(1-a)}{\omega r(1+a')} = \frac{(1-a)}{\lambda_r(1+a')}, \quad \lambda_r = \frac{\omega r}{V} \tag{11}$$

$$v = \sqrt{V^2(1-a)^2 + \omega^2 r^2(1+a')^2} \tag{12}$$

$$\alpha = \phi - \theta \tag{13}$$

Where ϕ is the flow angle, v the relative speed, α the AOA and θ the pitch angle. The flow angle ϕ is the angle between the relative speed and the plane of rotation whereas the AOA α is the angle between the relative speed and the chord of the blade element. The parameter V is the mean upstream wind velocity, ω the blade rotational speed and r the local radius of the blade element. The λ_r is the local TSR (Tip Speed Ratio) whereas the a and a' are the axial and tangential induction factors respectively. The a is the amount of reduction in axial wind speed when approaching the blade and a' the amount of rotational acceleration to blade because of the induced wake rotation. The terms $V(1-a)$ and $\omega r(1+a')$ are the effective axial wind and tangential blade speeds respectively.

Once the v, ϕ and α are estimated, the thrust and torque distribution around an annulus having width dr can be calculated as:

$$dT = \frac{1}{2} B\rho v^2 C_n c(r) dr \tag{14}$$

$$dQ = \frac{1}{2} B\rho v^2 C_t c(r) r dr \tag{15}$$

Where dT and dQ are the thrust and torque produced by the airfoil element in the annulus, B the number of blades, p the air density and $c(r)$ the local chord length. The C_n and C_t are the normal and tangential force coefficients which can be estimated from the relations:

$$C_n = C_L \cos\phi + C_D \sin\phi \tag{16}$$

$$C_t = C_L \sin\phi - C_D \cos\phi \tag{17}$$

Where C_L and C_D are the lift and drag coefficients which are taken as function of α either from static airfoil data table (in case of classical BEM) or estimated through model Equation (8) (in case of stochastic BEM).

To initialize the algorithm, induction factors can be guessed in start which in our case are taken as a=1/3 and a'=0. Later, the algorithm finds true values by iterative process using the relations given below. The axial induction factor is calculated either by relation suggested in basic BEM or modified Glauert correction model [31]. The basic BEM theory is effective up to axial induction factor of 0.4 which in other words up to thrust coefficient of 0.96. This assigns an upper limit for the validity of basic BEM theory. Beyond this point the wake breaks down and turbulent mixing occurs leading to highly transient and unpredictable state. In this state, the far wake propagates towards the upstream and causes an increase in turbulence violating the basic assumptions of the BEM theory. This causes deceleration of flow behind the rotor but the thrust continues to increase on the rotor [19]. To counter balance for this effect Buhl [31] introduced a relation by modifying Glauert correction model [32] to compute for axial induction factor when a>0.4. Higher axial induction means higher loading on the blade and vice versa. The loading condition in this context can be determined by:

$$C_T = 1 + \frac{\sigma(1-a)^2 C_n}{\sin^2\phi}, \sigma = \frac{Bc(r)}{2\pi r} \tag{18}$$

Where C_T is the thrust coefficient used in Equation (19) to estimate the axial induction factor by modified Glauert correction and σ the local solidity. When C_T>0.96F (for F see Equation (23)), the blade element is said to be highly loaded and the new axial induction factor will be estimated using modified Glauert correction model. Otherwise, in case $C_T \leq 0.96F$ the basic BEM method will be applied to estimate the axial induction factor. The relations used to calculate the true axial and tangential induction factors read:

$$a = \begin{cases} \dfrac{18F - 20 - 3\sqrt{C_T(50 - 36F) + 12F(3F - 4)}}{36F - 50} & \text{if } C_T > 0.96F \\ \left[1 + \dfrac{4F\sin^2\phi}{\sigma C_n}\right]^{-1} & \text{if } C_T \leq 0.96F \end{cases} \quad (19)$$

$$a' = \left[-1 + \frac{4F\sin\phi\cos\phi}{\sigma C_t}\right]^{-1} \quad (20)$$

Where F is the loss factor that represents the tip and root losses in combine and can be evaluated as:

$$F_{Tip} = \frac{2}{\pi}\cos^{-1}\exp\left[-\frac{B}{2}\frac{R_{Tip} - r}{r\sin\phi}\right] \quad (21)$$

$$F_{Root} = \frac{2}{\pi}\cos^{-1}\exp\left[-\frac{B}{2}\frac{r - R_{Root}}{r\sin\phi}\right] \quad (22)$$

$$F = F_{Tip}F_{Root} \quad (23)$$

The set of equations described in this section are iteratively solved for estimation of true axial and tangential induction factors. The process is repeated continuously (starting from Equation (11)) until the condition expressed in Equation (25) is fulfilled.

$$\begin{aligned} dif &= |a_{new} - a_{old}| \\ dif' &= |a'_{new} - a'_{old}| \end{aligned} \quad (24)$$

$$Condition \Rightarrow \begin{cases} Continue, & if\ Tol < dif\ and\ dif' \\ Stop, & if\ Tol \geq dif\ and\ dif' \end{cases} \quad (25)$$

Where *Tol* is the acceptable tolerance. The calculation converges to a tolerance value of 10^{-5} in our case.

4. RESULTS

The results are presented for rotor normal and tangential force coefficients acting on a blade element achieved with classical and stochastic BEM approaches. The force coefficients are obtained for AOAs 0-25° using Equations (16-17). This is done by varying TSR to change the inflow angle. The blade element is assumed to rotate at a constant local radius r=10m and constant pitch angle θ=3°. The local chord length and annular thickness are taken as $c(r)$=0.2m and dr=0.8m respectively. Moreover, at this preliminary stage the root and tip losses are ignored i.e. F=1.

The results for normal and tangential force coefficients are summarized in Figs. 2-3 respectively. The Fig. 2(a) and Fig. 3(a) show the $C_{n,Static}$ and $C_{t,Static}$ curves as function of AOA obtained with classical BEM. The Fig. 2(b) and Fig. 3(b) represent the $C_{n,Model}$ and $C_{t,Model}$ curves with local dynamics as function of AOA obtained with stochastic BEM.

In Fig. 2(b) and Fig. 3(b), the drift function obtained with Equation (4) presents the full map of local dynamics of the normal and tangential force coefficients for each AOA. Where, the red arrows display the deterministic increase of the normal and tangential force coefficients over the

time and the green arrows display the deterministic decrease of same parameters over the time. The black crosses represent the stable fix points matching the usual mean normal and tangential force coefficient curves where drift function is zero. The curve consisting of stable fix points (the black crosses) could be called Langevin normal and tangential force coefficient curves based on the approach used.

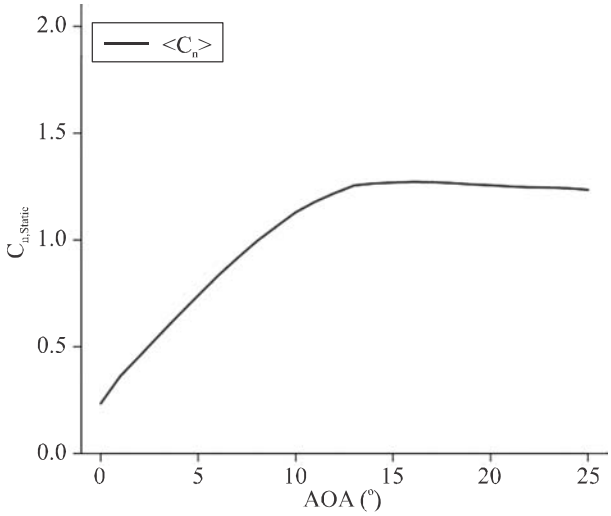

(a) $C_{n,Static}$ CURVE OBTAINED WITH CLASSICAL BEM

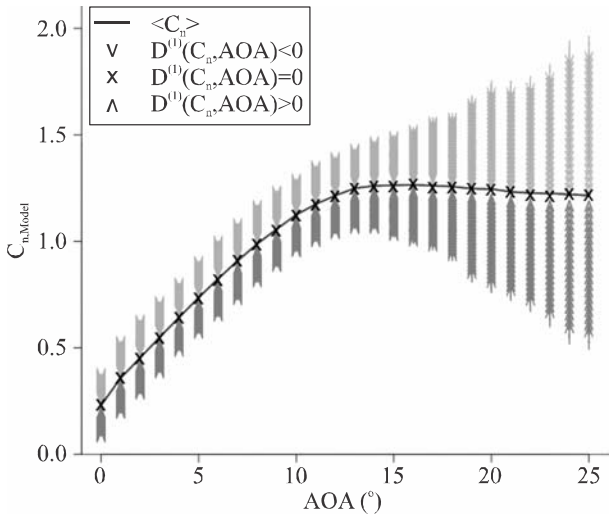

(b) $C_{n,Model}$ CURVE WITH LOCAL DYNAMICS OBTAINED WITH STOCHASTIC BEM. THE SOLID BLUE LINE REPRESENTS THE MEAN CURVE. THE RED AND GREEN ARROWS DEMONSTRATE THE POSITIVE AND NEGATIVE DRIFT FUNCTION TRYING TO MOVE TOWARDS THE STABLE FIX POINTS; THE BLACK CROSSES, WHERE DRIFT FUNCTION IS ZERO.

FIG. 2. NORMAL FORCE COEFFICIENT CURVES (COLOR ONLINE)

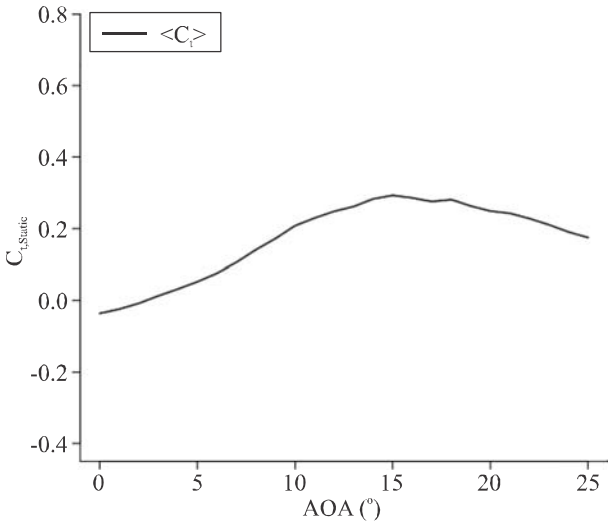

(a) $C_{t,Static}$ CURVE OBTAINED WITH CLASSICAL BEM

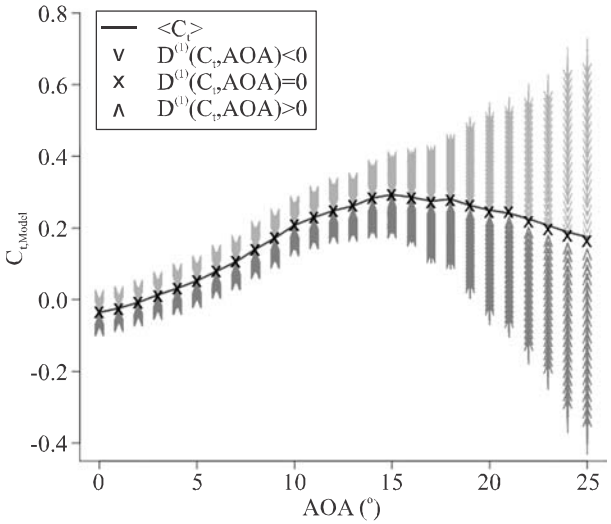

(b) $C_{t,Model}$ CURVE WITH LOCAL DYNAMICS OBTAINED WITH STOCHASTIC BEM. THE SOLID BLUE LINE REPRESENTS THE MEAN CURVE. THE RED AND GREEN ARROWS DEMONSTRATE THE POSITIVE AND NEGATIVE DRIFT FUNCTION TRYING TO MOVE TOWARDS THE STABLE FIX POINTS; THE BLACK CROSSES, WHERE THE DRIFT FUNCTION IS ZERO.

FIG. 3. TANGENTIAL FORCE COEFFICIENT CURVES (COLOR ONLINE)

The comparison of classical and stochastic BEM approaches in terms of their contributed results in Figs. 2-3 demonstrate that the classical BEM based on static tabulated airfoil data only provides the mean normal and tangential forces. In comparison to this, the stochastic BEM with integration of stochastic model brings additional insight by expressing complete map of the local force dynamics over the time. The mean curves of the normal and tangential force local dynamics show very good agreement with the mean curves obtained with classical BEM. The Langevin force coefficient curves shown in black crosses match almost perfectly with the mean of the normal and tangential force local dynamics.

5. CONCLUSIONS

A stochastic lift and drag model has been integrated to standard BEM model to achieve the dynamic forces on a rotating blade element. The forces are obtained with local dynamics for AOAs 0-25^{o} at constant local radius and constant pitch angle.

The comparison of classical and stochastic BEM approaches demonstrate that the stochastic BEM brings additional insight by expressing complete map of the local force dynamics over the time. The classical BEM based on static tabulated airfoil data only provides the mean forces. The mean curves of the local force dynamics show very good agreement with the mean curves obtained with classical BEM. The Langevin force curves shown in black crosses match almost perfectly with the mean curves of the local force dynamics.

The model is being developed to extract and provide the complete local loading information acting on the wind turbine blades which could lead to an optimum rotor design under turbulent wind circumstances. The final goal is to achieve an aerodynamic model like AeroDyn based on stochastic approach. Later it could be combined with a wind energy converter model like FAST or similar other model to obtain a stochastic rotor model.

ACKNOWLEDGEMENTS

The authors would like to thank Joerge Schneemann for access to his measured data. Also we would like to thank the referees for their helpful comments and suggestions for improvement of the paper.

REFERENCES

[1] Leishman, J.G., "Challenges in Modeling the Unsteady Aerodynamics of Wind Turbines", Wind Energy, Volume 5, Nos. 2-3, pp. 85-132, 2002.

[2] Morales, A., Waechter, M., and Peinke, J., "Characterization of Wind Turbulence by Higher Order Statistics", Wind Energy, Volume 15, No. 3, pp. 391-406, 2012.

[3] Boettcher, F., Barth, S., and Peinke, J., "Small and Large Scale Fluctuations in Atmospheric Wind Speeds", Stochastic Environmental Research and Risk Assessment, Volume 21, No. 3, pp. 299-308, 2007.

[4] Long, H., Wu, J., Mattew, F., and Tavner, P., "Fatigue Analysis of Wind Turbine Gear Box Bearings Using SCADA Data and Miner's Rule", Scientific Proceedings of EWEA, Brussels, Belgium, 2011.

[5] Muecke, T., Kleinhans, D., and Peinke, J., "Atmospheric Turbulence and its Influence on the Alternating Loads on Wind Turbines", Wind Energy, Volume 14, No. 2, pp. 301-316, 2011.

[6] Tangler, J.L., and Somers, D.M., "NREL Air Foil Families for HAWT's", Scientific Proceedings of AWEA, Washington DC, USA, January, 1995.

[7] Fuglsang, P., Antoniou, I., Dahl, K.S., and Madsen, H.A., "Wind Tunnel Tests of the FFA-W3-241, FFA-W3-301 and NACA 63-430 Airfoils", Scientific Report, Ris National Laboratory, No. Ris -R-1041(EN), Denmark, December, 1998.

[8] Fuglsang, P., Dahl, K.S., and Antoniou, I., "Wind Tunnel Tests of the Ris -A1-18, Ris -A1-21 and Ris -A1-24 Airfoils", Scientific Report, Ris National Laboratory, No. Ris -R-1112 (EN), Denmark, June, 1999.

[9] Timmer, W.A., and Van Rooij, R.P.J.O.M., "Summary of the Delft University Wind Turbine Dedicated Airfoils", Journal of Solar Energy Engineering, Volume 125, No. 4, pp. 488-496, 2003.

[10] Eggleston, D.M., and Stoddard, F.S., "Wind Turbine Engineering Design", Springer Publisher, 1st Edition, July 31, 1987.

[11] Leishman, J.G., "Principles of Helicopter Aerodynamics, Cambridge Aerospace Series", Cambridge University Press, 2nd Edition, April, 2006.

[12] Wolken-Moehlmann, G., Knebel, P., Barth, S., and Peinke, J., "Dynamic Lift Measurements on a FX79W151A Airfoil via Pressure Distribution on the Wind Tunnelwalls", Journal of Physics, Conference Series, Volume 75, No. 1, pp. 012026, 2007.

[13] Sant, T., "Improving BEM-Based Aerodynamic Models in Wind Turbine Design Codes", Phd Thesis, Delft University Wind Energy Research Institute, The Netherlands, 2007.

[14] Vermeera, L.J., Srensen, J.N., and Crespo, A., "Wind Turbine Wake Aerodynamics", Progress in Aerospace Sciences, Volume 39, Nos. 6-7, pp. 467-510, 2003.

[15] Conlisk, A.T., "Modern Helicopter Rotor Aerodynamics", Progress in Aerospace Sciences, Volume 37, No. 5, pp. 419-476, 2001.

[16] Snel, H., "Review of the Present Status of Rotor Aerodynamics", Wind Energy, Volume 1, No. S1, pp. 46-69, 1998.

[17] Ahlund, K., "Investigation of the NREL NASA/Ames Wind Turbine Aerodynamics Database", Scientific Report, Swedish Defence Research Agency, June, 2004.

[18] Hansen, M.O.L., and Madsen, H.A., "Review Paper on Wind Turbine Aerodynamics", Journal of Fluids Engineering, Volume 133, No. 11, pp. 114001, 2011.

[19] Moriarty, P.J., and Hansen, A.C., "AeroDyn Theory Manual", Technical Report, National Renewable Energy Laboratory, No. NREL/TP-500-36881, January, 2005.

[20] Weinzierl, G., "A BEM Based Simulation-Tool for Wind Turbine Blades with Active Flow Control Elements", Diploma thesis, Technical University of Berlin, 2011.

[21] Seoud, R.E., and Vassilicos, J.C., "Dissipation and Decay of Fractal-Generated Turbulence", Physics of Fluids, Volume 19, No. 10, pp. 105108, 2007.

[22] Schneemann, J., Knebel, P., Milan, P., and Peinke, J., "Lift Measurements in Unsteady Flow Conditions", Scientific Proceedings of EWEC, Warsaw, Poland, 2010.

[23] Risken, H., "The Fokker-Planck Equation", Springer Publisher, 2nd Edition, 1996.

[24] Siegert, S., Friedrich, R., and Peinke, J., "Analysis of Data Sets of Stochastic Systems", Physics Letters-A, Volume 243, Nos. 5-6, pp. 275-280, July, 1998.

[25] Kolmogorov, A.N., "Ueber Die Analytischen Methoden in Derwahrscheinlichkeitsrechnung", Mathematische Annalen, Volume 104, No. 1, pp. 415-458, 1931.

[26] Gottschall, J., and Peinke, J., "On the Definition and Handling of Different Drift and Diffusion Estimates", New Journal of Physics, Volume 10, No. 8, pp. 083034, 2008.

[27] Boettcher, F., Peinke, J., Kleinhans, D., Friedrich, R., Lind, P.G., and Haase, M., "Reconstruction of Complex Dynamical Systems Affected by Strong Measurement Noise", Physical Review Letters, Volume 97, No. 9, pp. 090603, 2006.

[28] Press, W.H., Teukolsky, S.A., Vetterling, W.T., and Flannery, B.P., "Numerical Recipes in C The Art of Scientific Computing", Cambridge University Press, 2nd Edition, 1992.

[29] Luhur, M.R., Waechter, M., and Peinke, J., "Stochastic Modeling of Lift and Drag Dynamics under Turbulent Conditions", Scientific Proceedings of EWEA, Copenhagen, Denmark, 2012.

[30] Burton, T., Sharpe, D., Jenkins, N., and Bossanyi, E., "Wind Energy Handbook", John Wiley & Sons, UK, 2002.

[31] Buhl, M.L.Jr., "A New Empirical Relationship between Thrust Coefficient and Induction Factor for the Turbulent Windmill State", Technical Report, National Renewable Energy Laboratory, No. NREL/TP-500-36834, August, 2005.

[32] Glauert, H., "A General Theory of the Autogyro", ARCR R&M No. 1111, 1926.

[33] Jonkman, M.J., Buhl M.L.Jr., "FAST User's Guide", Technical Report, National Renewable Energy Laboratory, No. NREL/EL-500-38230, August, 2005.